Reactive Power Reduction Method Based on Harmonics Analysis for Dual Active Bridge Converters with 3-Level Modulated Phase-Shift Control

Haochen Shi, Huiqing Wen, Jie Chen
Department of Electrical and Electronic Engineering
Xi'an Jiaotong-Liverpool University (XJTLU)
Suzhou, Jiangsu Province, China
Haochen. Shi@xjtlu.edu.cn

***Abstract*—This paper presents a novel reactive power minimization method under 3-level modulated phase-shift control in order to improve the efficiency for a wide range. Firstly a mathematic model of the DAB converter with 3-level modulated phase-shift control by a harmonic analysis method is obtained. Then, the detailed analysis of the odd order harmonic component of the active and reactive varied with the multiple control dimension is presented. On this basis, a novel optimal 3-level phase-shift control (OPS) strategy for reducing reactive power is proposed. Main simulation and experimental results by using the tradition method and the optimal reactive power reducing method are provided to verify the effectiveness of OPS method.**

Keywords—dual active bridge, phase shift, 3-level modulated control, reactive power,harmonic anlaysis

I. INTRODUCTION

The dual-active-bridge dc-dc converter has significant advantages in the voltage conversion system, because it can achieve high power density, bidirectional power flow ability, current isolation and soft switching. The most common control strategy is called the single-phase-shift (SPS), which only have a single phase shift between two sides of transformer. However, the reactive power, especially the backflow power will be very large when the voltage of primary and secondary is mismatched. It will lead to higher RMS current and power losses [1-5].

In order to overcome the weakness of the SPS, 3-level phase-shift modulated method is proposed to lower reactive power and RMS current [6-12]. Compared with SPS control, 3-level phase shift modulated strategy contains an additional inner phase shift between two switch pairs in each bridge, it create a 3-level wave instead of the square wave. It can dramatically improve the control flexible which lead to extend soft switching region and reduce backflow power to improve converter's efficiency. Based on the difference of inner phase shift mode, it can be divided into dual-phase-shift (DPS) control [6-8], extending-phase-shift (EPS) control [9-11], and triple-phase-shift (TPS) control [12].

The traditional theoretical approach to analyze the 3-level phase shift method is based on piecewise time domain model [1-11]. It can't be expressed by a single universal expression, because the inductor current in the different inner phase shift and operation states is variable in the time domain analysis. It significantly increase the difficulty of analyzing and designing 3-level phase shift methods. Moreover, it requires a simplified ideal inductive model of DAB converter to calculate a manipulable outcome[13].

Due to the complexity of the piecewise time domain expression, the optimal operation point is required a lot of complicated calculation, and the result is also a piecewise time domain function which is varied with different load and voltage conversion condition [14-19]. As the efficiency and current stress optimal method in the paper [18] and [19], the optimal point expression is too complex to do online calculations in the microchip, and it requires an offline parameter calculation to switch the optimal function to fit different operation states.

Based on the above analysis, a universal expression for 3-level modulated based on harmonic analysis is proposed. In this analytical model, the 3-level wave in each bridge is expressed as harmonic series forms. The inductor current is calculated from the second port network parameters and outer phase shift between two bridges. Then, the expression of active and reactive power with harmonic components are given. After that, the influence of variable order harmonic component on the current, active and reactive power is discussed. On this basis, an optimal reactive power eliminating control method include its theoretical analysis, simulation and experimental result is presented.

II. HARMONIC SERIES ANALYSIS OF 3-LEVEL PHASE-SHIFT MODULATED CONTROL

A. Typical 3-level modulation structure

The DAB converter illustrated in Fig. 1 can be seen as two-port network. The V_{B1} is the AC voltage of primary bridge and V_{B2} is the AC voltage of the secondary bridge refers to the primary side. The network N represents the network parameter for the two-port network. In this paper, the network N is considering as an ideal inductive network.

The waveform of 3-level phase-shift modulation is shown in the Fig. 2. The 3-level wave in each bridge is produced by inner phase shift of two switch pair in one bridge. It offer a benefit to reduce a circulating current by allowing circulating

978-1-4673-8888-7/16/$31.00 ©2016 IEEE

current inside bridge instead of backing to the input side. The angle α and β is inner phase angle for V_{B1} and V_{B2} side bridge

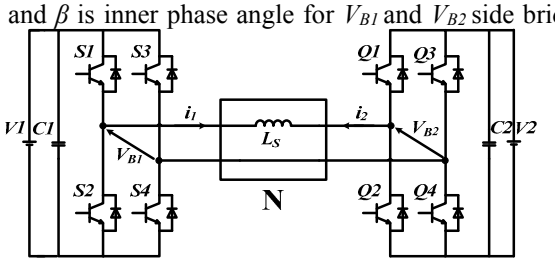

Fig. 1. Topology of DAB converter.

and i_1 and i_2 are the current for each bridge. The phase shift angle between two bridges is determined by the outer phase shift angle θ. The SPS control can be seen as a special case of the 3-level phase shift modulation when $\alpha=\beta=0$.

In order to simplify the universal expression, the 3-level wave should be symmetric structure [11]. Firstly, the starting point is the $i(t_0)=\alpha/2$, which allow a symmetric structure of 3-level wave in half cycle [20]. Then, the phase shift between two 3-level waves is δ, which is the angle between the central points of the each pulse wave. It indicates the influence of the inner phase shift α and β, as well as the outer phase shift θ. The relationship among the central point phase shift angle δ with inner and outer phase shifts is $\delta=\theta+(\alpha-\beta)/2$. Based on the condition above, the 3-level wave modulation could be described as a symmetric structure and significantly reduce the complexity of calculation.

B. Harmonic Series Form of Voltage and Current

According to the Fourier series, the 3-level square wave can be divide into combination of series odd order harmonics components. The AC link primary and secondary side voltage V_{B1} and V_{B2} can be rewritten as:

$$\begin{cases} V_{B1}=\sum\limits_{n=1,3,5,\ldots}\dfrac{4V_1}{n\pi}\cos(n\alpha/2) \\ V_{B2}=\sum\limits_{n=1,2,3,\ldots}\dfrac{4V_2}{n\pi}\cos(n\beta/2)\left[\cos(\delta)-j\sin(\delta)\right] \end{cases} \tag{1}$$

In the Fig. 1, the V_{B1} and V_{B2} can be seen a connected via simple two-port network. So the relationship between it is shown as:

$$\begin{bmatrix} I_1 \\ I_2 \end{bmatrix}=\begin{bmatrix} Y_{11} & Y_{12} \\ Y_{21} & Y_{22} \end{bmatrix}\begin{bmatrix} V_{B1} \\ V_{B2} \end{bmatrix} \tag{2}$$

where $[Y]$ is the admittance parameter matrix of the Network N. Considering the network N is seen as an ideal inductive network in this paper, the I_1 can be calculated from (1)-(2) is shown :

$$I_1=\sum_{n=1,3,5,\ldots}\frac{4}{n^2\pi\omega_0 L}\sqrt{A^2+B^2}\left[\cos\left(\arctan\frac{A}{B}\right)+j\sin\left(\arctan\frac{A}{B}\right)\right] \tag{3}$$

Where the $\omega_0=2\pi f_{sw}$, and

$$\begin{cases} A=V_2\cos(n\beta/2)\cos(n\delta)-V_1\cos(n\alpha/2) \\ B=V_2\cos(n\beta/2)\cos(n\delta) \end{cases} \tag{4}$$

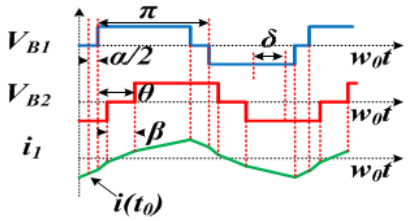

Fig. 2. The waveform of the 3-level modulated phase shift method

By the (1) – (4), the AC link voltage and inductor current in the different operation condition of the 3-level modulated phase shift method can be described by a universal expression as combination of the series odd order harmonics component. It can significantly simplify the complexity of the DAB mathematical model than traditional piecewise expression.

C. Harmonic Series Forms of Active Power

The active power for the AC link voltage and current for DAB can be described as

$$P=UI\cos(\varphi) \tag{5}$$

Where the power factor $\cos(\varphi)$ is used to indicate the phase differences between the voltage and current. Due to the both voltage and current are harmonic series form, the power factor can be divided into two situations: 1) the power factor for the current and voltage in the same order harmonic component, the power factor is follow its definition. 2) The power factor for voltage and current in different order is equal to 0 due to the orthogonality of trigonometric function. So we have

$$\begin{aligned} \cos(\varphi)_n &= \cos(-\arctan\frac{A}{B}) \\ \cos(\varphi)_{m\neq n} &= 0 \end{aligned} \tag{6}$$

Taking this condition into the (1) - (4), we have

$$\begin{aligned} P &= \sum_{n=1,3,5,\ldots}\frac{8V_1\sqrt{A^2+B^2}}{n^3\pi^2\omega_0 L}\cos(n\alpha/2)\cos\left(-\arctan\frac{A}{B}\right) \\ &= \sum_{n=1,3,5,\ldots}\frac{8V_1V_2}{n^3\pi^2\omega_0 L}\cos(n\alpha/2)\cos(n\beta/2)\sin(n\delta) \end{aligned} \tag{7}$$

The active power can be normalized by the unified power $P_N=V_1*V_2/(8f_s*L)$ .The Fig. 3(a) gives the change of the unified active power in different order component along with the change of angle δ. The active power in all order components is axis symmetry around $\delta=\pi/2$. It can be seen that the fundamental components of active power is taking charge of the active power, and it conform to the active power in the piecewise time domain model. It proves that the fundamental components of active power can be used to represent the active power with sustainable error.

D. Harmonic Series Forms of Reactive Power

Due to the phase difference between the ac voltage and

current, the DAB converter is also contain a reactive power.

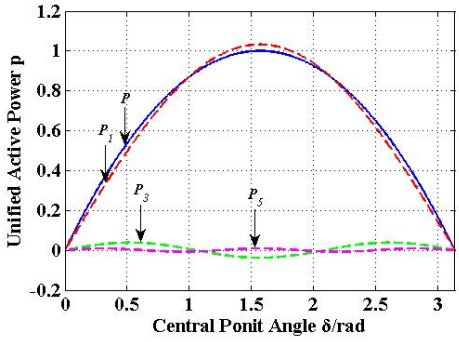

(a)

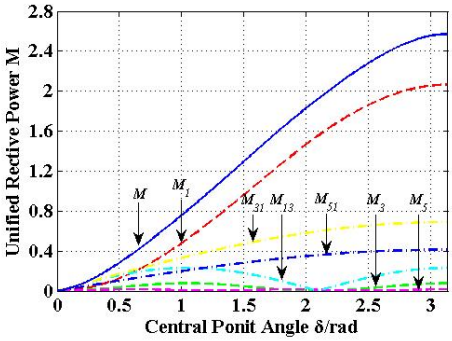

(b)

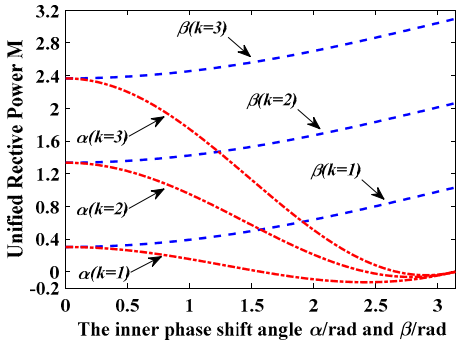

(c)

Fig. 3. (a)The active power of DAB vaired with central point angle δ.(b) The reactive power of DAB vaired with central point angle δ.(c) The reactive power of DAB varied with α, β and k.

The reactive power of the DAB can be described as

$$Q = UI\sin(\varphi) \tag{8}$$

Compared with the active power, the reactive power is not only occurring between the same order voltage and current, but also cause by the different order component. So the reactive power can be derived as follow

$$\begin{aligned} Q_n &= \sum_{n=1,3,5,..} \frac{8V_1\sqrt{A^2+B^2}}{n^3\pi^2\omega_0 L}\cos(n\alpha/2)\sin\left(-\arctan\frac{A}{B}\right) \\ &= \sum_{n=1,3,5,..} \frac{8V_1}{n^3\pi^2\omega_0 L}\left[V_1\cos^2(n\alpha/2)\right. \\ &\left. -V_1V_2\cos(n\alpha/2)\cos(n\beta/2)\cos(n\delta)\right] \end{aligned} \tag{9}$$

and the mismatch order reactive power

$$Q_{m\neq n} = U_m I_n = \sum_{n=1,3,5,..} \frac{8V_1\sqrt{A^2+B^2}}{mn^2\pi^2\omega_0 L}\cos(m\alpha/2) \tag{10}$$

The Fig. 3(b) shows the relationship between the reactive power and angle δ. It is clear that the reactive power in the increases along with the rising of the δ, while first order components of reactive power also has the largest value among all odd order components. The reactive power caused by the first order current with different order voltage is also higher than the other odd order component, because the attenuation is n times less than higher order component. But the changing of it is as same as the fundamental component which can be also represented by it. So the series of odd order harmonic reactive power can be described by the first order harmonic component.

The relationship of the unified reactive power varied with primary and secondary inner phase shift angle α and β are shown in the Fig. 3(c) when outer phase shift angle $\delta=\pi/4$. The voltage conversion ratio $k= V_1/V_2$, and we assume the $k \geq 1$ in the fig.3, the boost mode $k < 1$ can be analyzed similarly. It's clearly that the higher inner phase shift angle β and k are lead to the higher reactive power. For the variable α, higher k cause higher initial reactive power, and the reactive power is firstly decreasing along with the increasing α below the zero, and then increasing to the zero when the $\alpha=\pi$. The negative reactive power is the opposite direction reactive power in the AC link circuit. So it can be seen that the reactive power could reach zero reactive power twice in the whole α changing region.

III. Reactive Power Optimal Control Strategy

A. Optimal Control Strategy to Reduce Reactive Power

Based on the analysis above, the first order harmonic component is not only contribute to the main part of the active and reactive in the DAB, but also follow the change trend of it. So the first order harmonic component can be chosen to optimize their reactive power.

From the Fig. 3(a) and (b), the active power is symmetry around $\delta = \pi/2$, while the reactive power is monotone increasing with δ. In order to achieve the less reactive power the central point angle need to be limited in $\delta \in [0, \pi/2]$ .After that, the normalized first order component of the reactive power from (9) is

$$M_1 = \frac{32}{\pi^3 V_2}\cos(n\alpha/2)\left[V_1\cos(n\alpha/2) - V_2\cos(n\beta/2)\cos(n\delta)\right] \tag{11}$$

In order to obtain the minimum reactive power with required active power, the Lagrange multiplier method (LMM) is common method which can be described as

$$L = M_1 + \lambda(p - p_0) \tag{12}$$

Where L is the Lagrangian function, λ is the Lagrangian multiplier and p_0 is the required active power. The LLM method need to follow the condition below

$$\begin{cases} \dfrac{\partial L}{\partial \alpha}=0, \dfrac{\partial L}{\partial \beta}=0, \dfrac{\partial L}{\partial \delta}=0 \end{cases} \tag{13}$$

From the (11)-(13), the result of the LLM is the boundary condition for minimum reactive power operation. So the result of the (13) can be rewritten as

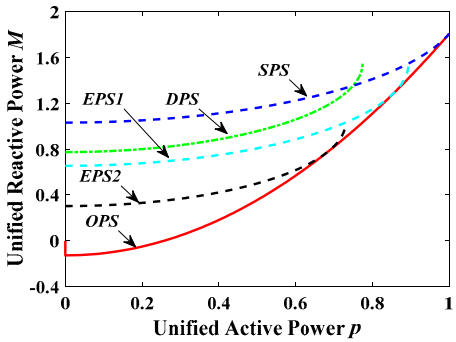

(a)

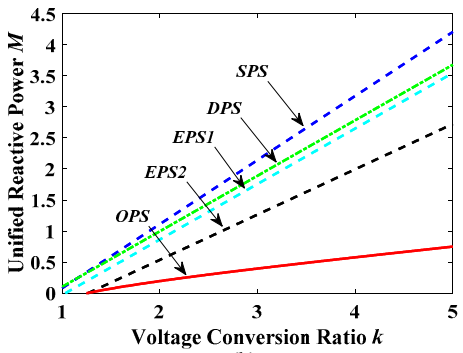

(b)

Fig. 4. (a)The reactive power of DAB vaired with central point angle δ.(b) The reactive power of DAB varied with α, β and k.

$$\begin{cases} \alpha = 2\arccos\left(\sqrt{1/4k^2+\pi^6 p_0^2/1024}\right) \\ \beta = 0 \\ \delta = \arctan\left(kp_0\pi^2/16\right) \end{cases} \tag{14}$$

Due to limitation of the trigonometric function, it requires

$$\sqrt{1/4k^2+\pi^6 p_0^2/1024} \le 1 \tag{15}$$

According to the (14) and (15), as well as the analysis below, the range of the p_0 are

$$p_0 \in \left[0, \frac{1024}{\pi^6}\sqrt{1-\frac{1}{4k^2}}\right] \tag{16}$$

From the (16), it can be seen that the maximum value of the active power is determined by the k. In this paper, we assume k>1. For the smallest condition that k=1,the maximum value $p_{\max} \approx 0.92$,which can generally be seen as covering all load range with tolerable error, while the higher k will lead to higher reactive power. So OPS control can ensure the maximum power transmission ability like the SPS control, which increasing its operational load range.

B. Comparsion analysis of the OPS

The Fig. 4(a) is the comparison analysis among the different phase shift control method about the unified reactive power M varied with the unified power p. The EPS1 is for the $\alpha=\pi/3$, $\beta=0$, the EPS2 is for $\alpha=\pi/2$, $\beta=0$, the DPS is for $\alpha=\pi/3$, $\beta=\pi/3$, and the SPS is for $\alpha=0$, $\beta=0$. It is clearly that the higher active power will lead to higher reactive

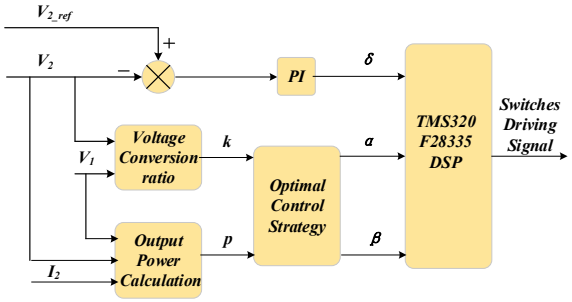

Fig. 5. The control scheme of the proposed method

for all control method, while the EPS1, EPS2, DPS and OPS are dramatically has lower reactive power than the SPS control. It also show that the inner phase shift angle α and β are lead to smaller maximum transmission power than the SPS and OPS control.

Comparison among the EPS1, EPS2 and DPS show the larger primary inner phase shift angle α can cause lower reactive power with same transmission active power, and secondary inner phase shift angle β in the DPS control show negative influence on the reducing reactive power and maximum transmission power. In all control methods in the figure, the OPS control method has the lowest reactive power and can nearly cover all load region.

C. Control scheme of the proposed method

The control scheme for the OPS control is proposed in the Fig. 5. The outer phase shift angle δ is controlled by the PI controller to ensure the close loop control of the DAB. In order to apply the OPS control method, the voltage conversion ratio k and unified power p can be calculated by the input/output voltage and output current which is measured by the current and voltage sensor. The inner phase shift angle α and β can be gained by the (14), which is used to adjust the reactive power. The α, β and δ is sent into the DSP TMS320F28335 and transferred to 16 driving signals for 8 switches in two bridge.

IV. Experimetal Results

The 200W prototype of the DAB converter is built to verify the theoretical and simulation analysis, which the auxiliary inductor $L=150\mu H$, the switching frequency $f_s=20kHz$, and input voltage $V_1=80V$ and the output voltage refer to the input side $V_2=64V$, the turns ratio of the transformer $N=1:2$, so the output terminal voltage $V_{2dc}=128V$.

The simulation result in the Fig. 6 (a) and (b) shows the OPS control method can eliminate the additional reactive power or backflow power existed in the SPS control method. It is clearly that the reactive current will back flow into the power supply during the red area in the SPS control, while the reverse direction current in the OPS control is circulating inside the primary bridge due to the inner phase difference between two active bridge arms. Because the backflow power is a part of the reactive power, so the reactive power is lower in the OPS control. For the OPS control, the traditional outer phase shift can be seen as 0, while the central point outer phase shift is not, so the transmission power is higher than

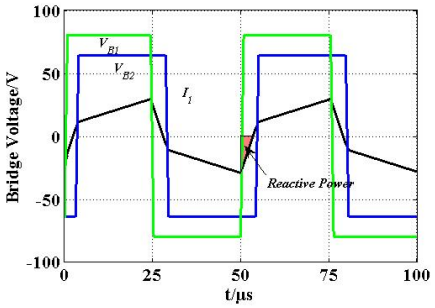

(a)

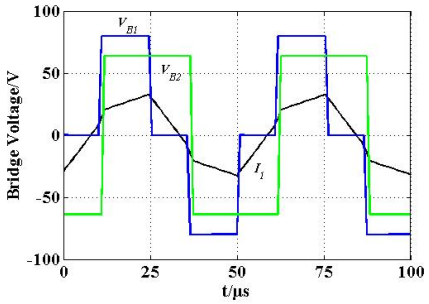

(b)

Fig. 6. (a)Simulation waveform of the SPS contorl with V_1=80V, V_2=64V and p=0.6.(b) Simulation waveform of the OPS contorl with V_1=80V, V_2=64V and p=0.6.

zero, which indicate that the traditional outer phase shift control is not suitable for the 3-level modulated phase shift control. The experimental waveform in the Fig. 7(a) and (b) are the DAB porotype operating under the same condition, due to hardware limitation, the secondary side measurement is taking the V_{2dc} instead of V_2, and it verifier the simulation result.

The comparison among the efficiency of SPS, EPS and OPS varied with the transmission power is shown in the Fig. 8(a). It can be seen that efficiency of all control method is increasing along with the transmission power, while the OPS control has the highest efficiency in all load conditions. Compared with the SPS control, both EPS and SPS control can be useful for improving the efficiency of the DAB converter. The EPS control has lower efficient in the light load condition, but it can also achieve the highest efficiency in the heavy load condition, which is following the reactive power analysis above.

In order to investigate influence of the voltage conversion ratio k, the SPS, EPS and OPS control under changing of the input voltage V_1 is shown in the Fig. 8(b). The output voltage is stable at 128V and transmission power is equal to 75W in all condition. The comparison among the efficiency of SPS, EPS and OPS varied with the transmission power is shown in the Fig. 7(a). The increasing of the input voltage lead to rapidly decrease of the efficiency in the SPS control, while the decrease of the efficiency for OPS and EPS control is much slower. Compared with the efficiency difference between EPS and OPS control in the initial condition, the efficiency difference is larger in the V_1=110V condition, which indicate the OPS can gain higher efficiency with higher voltage conversion ratio k. Based on those figure and experimental waveform, it shows that OPS control can effectively reduce the reactive power, especially in the light load and high voltage conversion condition.

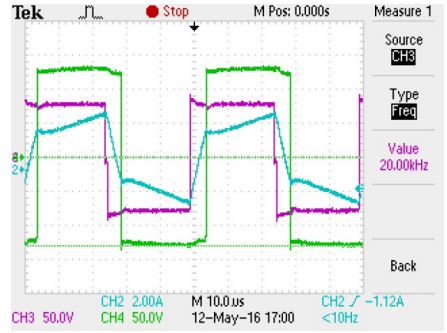

(a)

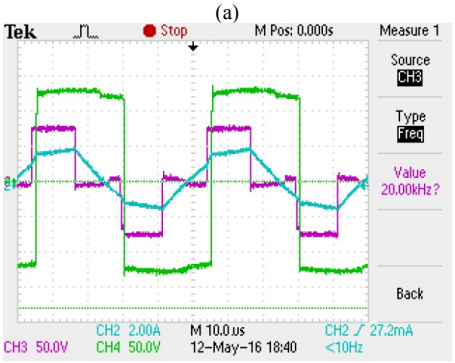

(b)

Fig. 7. (a) Experiment waveform of the SPS contorl with V_1=80V, V_{2dc}=128V and p=0.6.(b) Experiment waveform of the OPS contorl with V_1=80V, V_{2dc}=128V and p=0.6.

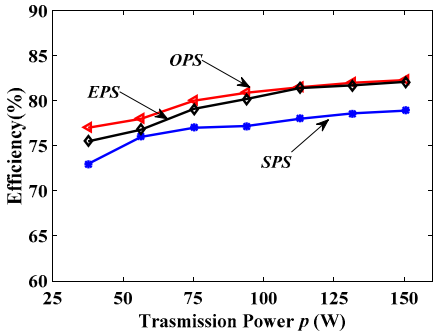

(a)

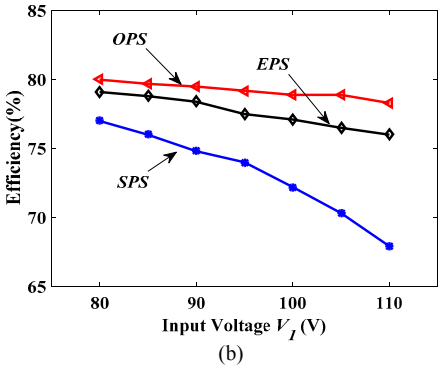

(b)

Fig. 8. (a)Efficiency of SPS,EPS and OPS when V_1=80V, V_{2dc}=128V varied with transmission power p.(b)Efficiency of SPS,EPS and OPS when p=75W, V_{2dc}=128V varied with input voltage V_1.

V. CONCLUSION

A novel reactive power reduction method under 3-level modulated phase shift control is proposed in this paper. According to the universal fundamental reactive power expression from harmonics analysis and LMM, the reactive power can be maintained at the lowest in all load range. Then, the comparison SPS, EPS and DPS is confirmed that the OPS can also guarantee the minimum reactive power and maximum active power transmission ability during voltage conversion ratio variation. The reduction of the reactive power can dramatically decrease losses of the DAB and improve its efficiency. Furthermore, the optimal algorithm under harmonics analysis in this paper can significantly easier for implemented on the microcontroller, because it can avoid multiple modes selection by voltage conversion ratio or transmission power in the traditional piecewise time domain algorithm.

VI. ACKNOWLEDGEMENT

This research was supported by the University Fund (TDF 14/15-R10-083), the State Key Laboratory of of Power Transmission Equipment & System Security and New Technology (2007DA10512716414), the Jiangsu Science and Technology Programme (BK20161252), and the National Nature Science Foundation of China (51407145).

REFERENCES

[1] C. Mi, H. Bai, C. Wang *et al.*, "Operation, design and control of dual H-bridge-based isolated bidirectional DC–DC converter," *IET Power Electronics,* vol. 1, no. 4, pp. 507, 2008.

[2] Wen, H.; Su, B.; Xiao, W., "Design and performance evaluation of a bidirectional isolated dc-dc converter with extended dual-phaseshift scheme," IET Power Electron., vol.6, no.5, pp.914-924, May 2013.

[3] F. Krismer, and J. W. Kolar, "Accurate Power Loss Model Derivation of a High-Current Dual Active Bridge Converter for an Automotive Application," *IEEE Transactions on Industrial Electronics,* vol. 57, no. 3, pp. 881-891, 2010.

[4] Huiqing Wen; Weidong Xiao; Bin Su, "Nonactive Power Loss Minimization in a Bidirectional Isolated DC–DC Converter for Distributed Power Systems," IEEE Trans. Ind. Electron., vol.61, no.12, pp.6822-6831, Dec. 2014.

[5] Wen H, Su B., "Operating modes and practical power flow analysis of bidirectional isolated power interface for distributed power systems," Energy Conversion and Management, vol. 111, pp. 229-238, 2016.

[6] H. Bai, Z. Nie, and C. C. Mi, "Experimental Comparison of Traditional Phase-Shift, Dual-Phase-Shift, and Model-Based Control of Isolated Bidirectional DC-DC Converters," *IEEE Transactions on Power Electronics,* vol. 25, no. 6, pp. 1444-1449, 2010.

[7] H. Bai, and C. Mi, "Eliminate Reactive Power and Increase System Efficiency of Isolated Bidirectional Dual-Active-Bridge DC-DC Converters Using Novel Dual-Phase-Shift Control," *IEEE Transactions on Power Electronics,* vol. 23, no. 6, pp. 2905-2914, 2008.

[8] B. Zhao, Q. Song, and W. Liu, "Power Characterization of Isolated Bidirectional Dual-Active-Bridge DC-DC Converter With Dual-Phase-Shift Control," *IEEE Transactions on Power Electronics,* vol. 27, no. 9, pp. 4172-4176, 2012.

[9] B. Zhao, Q. Yu, and W. Sun, "Extended-Phase-Shift Control of Isolated Bidirectional DC-DC Converter for Power Distribution in Microgrid," *IEEE Transactions on Power Electronics,* vol. 27, no. 11, pp. 4667-4680, 2012.

[10] G. Oggier, G. O. Garc, A. R. Oliva *et al.*, "Modulation strategy to operate the dual active bridge DC-DC converter under soft switching in the whole operating range," *IEEE Transactions on Power Electronics,* vol. 26, no. 4, pp. 1228-1236, 2011.

[11] A. K. Jain, and R. Ayyanar, "Pwm control of dual active bridge: Comprehensive analysis and experimental verification," *IEEE Transactions on Power Electronics,* vol. 26, no. 4, pp. 1215-1227, 2011.

[12] K. Wu, C. W. d. Silva, and W. G. Dunford, "Stability Analysis of Isolated Bidirectional Dual Active Full-Bridge DC-DC Converter With Triple Phase-Shift Control," *IEEE Transactions on Power Electronics,* vol. 27, no. 4, pp. 2007-2017, 2012.

[13] A. Rodr, A. Vazq, guez *et al.*, "Different Purpose Design Strategies and Techniques to Improve the Performance of a Dual Active Bridge With Phase-Shift Control," *IEEE Transactions on Power Electronics,* vol. 30, no. 2, pp. 790-804, 2015.

[14] F. Krismer, and J. W. Kolar, "Closed Form Solution for Minimum Conduction Loss Modulation of DAB Converters," *IEEE Transactions on Power Electronics,* vol. 27, no. 1, pp. 174-188, 2012.

[15] G. G. Oggier, G. O. Garc, and A. R. Oliva, "Switching Control Strategy to Minimize Dual Active Bridge Converter Losses," *IEEE Transactions on Power Electronics,* vol. 24, no. 7, pp. 1826-1838, 2009.

[16] N. Hou, W. Song, and w. m, "Minimum-Current-Stress Scheme of Dual Active Bridge DC-DC Converter With Unified-phase-shift Control," *IEEE Transactions on Power Electronics,* vol. PP, no. 99, pp. 1-1, 2016.

[17] B. Zhao, Q. Song, W. Liu *et al.*, "A Synthetic Discrete Design Methodology of High-Frequency Isolated Bidirectional DC/DC Converter for Grid-Connected Battery Energy Storage System Using Advanced Components," *IEEE Transactions on Industrial Electronics,* vol. 61, no. 10, pp. 5402-5410, 2014.

[18] B. Zhao, Q. Song, W. Liu *et al.*, "Current-Stress-Optimized Switching Strategy of Isolated Bidirectional DC-DC Converter With Dual-Phase-Shift Control," *IEEE Transactions on Industrial Electronics,* vol. 60, no. 10, pp. 4458-4467, 2013.

[19] B. Zhao, Q. Song, and W. Liu, "Efficiency Characterization and Optimization of Isolated Bidirectional DC-DC Converter Based on Dual-Phase-Shift Control for DC Distribution Application," *IEEE Transactions on Power Electronics,* vol. 28, no. 4, pp. 1711-1727, 2013.

[20] B. Zhao, Q. Song, W. Liu *et al.*, "Universal High-Frequency-Link Characterization and Practical Fundamental-Optimal Strategy for Dual-Active-Bridge DC-DC Converter Under PWM Plus Phase-Shift Control," *IEEE Transactions on Power Electronics,* vol. 30, no. 12, pp. 6488-6494, 2015.